AGU100 ADVANCING EARTH AND SPACE SCIENCE

Earth and Space Science

RESEARCH ARTICLE
10.1029/2019EA000584

Weakening of Triennial Oscillation of the Indian Summer Monsoon Rainfall (at 1° × 1° Gridded Scale) Under Future Global Warming

Pravat Jena[1] **and Sarita Azad**[1]

[1]School of Basic Sciences, Indian Institute of Technology, Mandi, Kamand, India

Key Points:

- This study analyzes the spatial distribution of triennial oscillation of Indian summer monsoon rainfall
- The amplitude of the triennial oscillation is projected to be weakening in future under the RCP 8.5 scenario
- One-to-one correspondence between time and frequency domain is established

Correspondence to:
S. Azad,
sarita@iitmandi.ac.in

Citation:
Jena, P., & Azad, S. (2019). Weakening of triennial oscillation of the Indian summer monsoon rainfall (at 1° × 1° gridded scale) under future global warming. *Earth and Space Science*, *6*, 1262–1272. https://doi.org/10.1029/2019EA000584

Received 4 FEB 2019
Accepted 4 JUN 2019
Accepted article online 8 JUL 2019
Published online 25 JUL 2019

Abstract India's agriculture is a significant component of the Gross National Product (GNP) and is largely dependent on the Indian summer monsoon. This makes an accurate prediction of rainfall a key factor in improving agricultural production. A statistical cycle, widely known to have a strong 2.85-year period and will therefore be called a triennial oscillation here, plays a vital role in such predictions. In the present work, we examine the spatial distribution of this short-period oscillation at 1° × 1° (lat./long.) resolution using 1,260-month data (1901–2005). A power spectral analysis of the observed data set shows that the statistically significant triennial oscillation (at 95% confidence level) is present over 54% of the total number of 354 grids across India, which covers 69.03% area. Projections of selected data from models used in Coupled-Model Inter-comparison Project Phase 5 predict weakening of this oscillation (in amplitude) by 2100. The projections indicate reduced confidence levels of this oscillation at 80%, 85%, and 90%, respectively, in 3%, 20%, and 62% of the selected 54% grids, which covers 41.3% area. A weakened triennial monsoon cycle will have a severe impact on agriculture and water resource management, particularly over the southwest-coastal, northern, and northeast-central parts of India.

Plain Language Summary An accurate prediction of Indian monsoon rainfall is of utmost importance for many applications like agriculture, water resource management, and extreme events. One of the ways to assess the degree of predictability in the monsoons is by extracting the significant oscillations present in the given data. This work evaluates the presence of triennial oscillation for this purpose and assesses the changes in its magnitude in future projections. The results reveal that the significance levels of this oscillation are decreasing over a large part of the country.

1. Introduction

The Indian monsoons interact and operate over a broad range of temporal and spatial scales. In spite of this complexity, rainfall data specifically show well-defined patterns, and a large number of studies suggest that the Indian summer monsoon rainfall (ISMR) has a 95% significant periodicity of 2.85 years, which has been detected using both linear and nonlinear techniques (Azad & Narasimha, 2008; Iyengar & Kanth, 2005; Kailas & Narasimha, 2000; Kumar, 1997). The established 2.85-year periodicity of ISMR has been known to be a significant component of the tropical "biennial" oscillation (Mooley & Parthasarathy, 1984). The tropical biennial oscillation is generally defined as the tendency for the monsoon to switch between "strong" and "weak" years (Loschnigg et al., 2003; Meehl, 1987; Meehl, 1997). A relatively strong monsoon is said to occur during year i as when the following relation holds (Meehl & Arblaster, 2002; Meehl et al., 2003):

$$x_{i-1}<x_i>x_{i+1}. \tag{1}$$

Similarly, a weak year i is defined by the relation

$$x_{i-1}>x_i<x_{i+1}. \tag{2}$$

In fact, variability in the ISMR has been found to be characterized by several cycles in the spectrum, which includes oscillations in the band of 2- to 3-, 3- to 5-, 5- to 10-, and 10- to 20-year periods (Azad & Narasimha, 2008; Azad et al., 2007; Azad et al., 2010; Kailas & Narasimha, 2000; Kumar, 1997). Besides these periodicities, Indian monsoon has teleconnection with the global phenomenon widely known as El Niño Southern Oscillation (ENSO) in 3 to 5-year period band (Narasimha & Bhattacharya, 2010). In a recent work by the

authors (Azad & Rajeevan, 2016), it was shown that the inverse relation of rainfall-ENSO in 3- to 5-year band is probable to shift to shorter periods (3–2.5 years) in future, leading to assumption about possible weakening of the triennial oscillation of the ISMR. Therefore, in this work we focus on the triennial oscillation, its spatial distribution, and how it is likely to change in future simulations of Coupled-Model Inter-comparison Project Phase 5 (CMIP5).

General circulation models (GCMs) are generally used for deriving future simulations of climate. The fifth assessment report of Intergovernmental Panel on Climate Change provides coupled models of CMIP5 to assess future climate change scenarios. Due to the availability of projections from these models (Taylor et al., 2012), there had been a great attention in evaluating the changes in ISMR under projected warming. Apart from some uncertainties in the models (Knutti & Sedláček, 2013; Liu et al., 2015; Loschnigg et al., 2003; Sengupta & Rajeevan, 2013), it was found that the CMIP5 models satisfactorily replicate the dominant features of the monsoons and changes in mean rainfall, annual cycle extreme events, Walker Circulation, and so forth have been reported (Feng et al., 2013; Jena et al., 2015, 2016; Kociuba & Power, 2015; Menon et al., 2013).

The evidence of changes in the triennial oscillation would be useful for policy makers, farmers, water managers, and so forth. In a predominantly agricultural country like India, weak and strong monsoons substantially alter agricultural output, and thus also the economy of the country (Chaudhari et al., 2010; Kripalani et al., 2003; Mooley & Parthasarathy, 1984). Therefore, reliable prediction of this oscillation has immense importance for agricultural activities and water resource management.

The paper is divided into three different sections. The observed and GCMs' data sets with methodology are mentioned in section 2. Section 3 gives the details on the analysis of the results, and a concluding remark is described in section 4 followed by the reference part, which is mentioned in section 5.

2. Data and Methodology

2.1. Data

The gridded rainfall data of 1° × 1° (1° latitude = 110.56 km. at equator) spatial resolution, spanning over the period of 1901–2005, were obtained from the open web repository of climatic research unit, UK (http://www.cru.uea.ac.uk; Harris et al., 2014) to facilitate the study. The spatial domain for analysis comprised of 354 grids and was chosen to be in the range of latitude 8°4′ to 37°5′ and longitude 68°5′ to 97°5′ covering the Indian region. To focus on ISMR, monthly data from June to September (JJAS) in each year were adopted to constitute the 105-year rainfall time series for each of the 354 grids. Furthermore, all-India JJAS time series were obtained by taking the area-weighted average of all grids using a standard weighted matrix (Rajeevan et al., 2006) provided by the Indian Meteorological Department—the national meteorological agency of India.

The present study analyzes historical simulations (1901–2005) as well as future projections for rainfall of 28 CMIP5 and 20 climate models for ENSO (2006–2100) under the RCP8.5 scenario (Taylor et al., 2012). Using the bilinear interpolation technique, the GCM outputs are rescaled to the observed data resolution of 1° × 1°. Bilinear interpolation provides a good representation of data without relegating the quality and is adequate for many applications. Other interpolation techniques like Budget and nearest neighbor are demonstrated only for the high-resolution grid transformation by Accadia et al. (2003). It has been reported that precipitation forecasts show greater spatial variability and strong gradients at higher resolution. Verification (and intercomparison) of mesoscale models on a coarser grid should be less sensitive to small forecast displacements errors. Therefore, the present analysis has been conducted on the coarse grid transformations of models, and in such cases, bilinear method provides good results (Spicer et al., 2009; Yoon et al., 2012).

2.2. Methodology

The fast Fourier transform is employed to obtain the power spectral density (PSD) of a stationary random process. The spectral representation of a discrete time series $x(t)$ with unit time interval is known to be a periodogram defined as (Stoica & Moses, 1997)

$$x(\omega_k) = \frac{2}{N}\left|\sum_{t=0}^{N-1} x(t)e^{-i\omega_k t}\right|^2, \quad (3)$$

in which $\omega_k = 2\Pi k/N$, N is the sample size, and $k = 0,1,...,N/2$ is the frequency index. The Welch technique uses the technique of hamming window to extract the energy $x(\omega_k)$ of the frequency. In order to reduce the variance induced by the standard periodogram, the method uses the concept of averaged periodogram of overlapped, windowed segments of a time series. The average periodogram is obtained by applying equation (3) in each part of overlapped partition data and averaging over the periodogram.

The peak obtained in the spectrum undergoes a statistical significance test, which needs a finite reference discrete time series. For this purpose, the first-order autoregressive is used, which is defined as

$$X(t) = \alpha X(t-1) + \varepsilon(t), \quad (4)$$

whose normalized PSD function is

$$P_k = \frac{1-\alpha^2}{1+\alpha^2-2\,\alpha cos\left(\frac{2\pi k}{N}\right)}, \quad (5)$$

where $k = 0,1,...,N/2$ is the frequency index and $t = 1,...,N$ denotes discrete time in units of the sampling interval. For $t = 1$, $X(1) = \alpha \times 0 + \varepsilon(1)$, where $X(0) = 0$ is the lag-1 autocorrelation coefficient ($0 < \alpha < 1$) and $\varepsilon(t)$ is a Gaussian white noise process with mean zero and an appropriate variance. From equation (5), it is clear that the shape of the spectrum P_k varies according to the value of α. Moreover, it is seen that (Azad et al., 2007) the value of α depends on the data. For rainfall it is close to zero; hence, the spectrum takes the shape of white noise.

If a peak in the power spectrum is significantly above this background spectrum (Gilman et al., 1963), then it is a result of statistical fluctuation, which can be subjected to the test with a specified confidence level. To obtain the confidence level, the reference spectrum is multiplied with 95% percentile value of chi-square distribution with 2 degrees of freedom. Then after, the peak exceeds, the 95% percentile is extracted and treated as statistically significant cycle.

3. Results and Discussion

The PSD of the JJAS series is estimated and shown in Figure 1a against a background spectrum. The significance test on the PSD of rainfall data shows 2.85 years, which is significant at 95% confidence level (henceforth referred to as triennial oscillation). It is observed in Figure 1a that the rainfall spectrum has relatively significant power at lower and higher frequencies. It has been proved that there is a statistical significant spectral dip in a band around the 4-year period (0.25 year^{-1}) and not a mere random fluctuation (Azad et al., 2010). Furthermore, in a recent work by the authors (Azad & Rajeevan, 2016), it was shown that this spectral dip in the 3- to 5-year (0.3–0.2 (1/year)) band indicates a rainfall-ENSO inverse relation and is likely to shift to shorter periods (3–2.5 years) in future, speculating a possible weakening of the triennial oscillation of the Indian monsoon rainfall.

In Figure 1b, the significant 2.85-year period (at 95% confidence level) is estimated spatially over the Indian mainland. It is shown that out of the total 354 grids, the significant triennial oscillation exists in 191 grids, which is 53.9% of the total grids. Moreover, the region of northeast-central, west coast, and northern part of the country are seen to form dense clusters of the significant triennial oscillation.

To investigate future projections of the triennial oscillation, first, the CMIP5 models in the historical time period (1901–2005) are selected. Selection of optimum models is usually performed by considering the spatial matching of models with the observed data. The PSD function is implemented for CMIP5 hindcast-gridded data sets to visualize the distribution of triennial oscillation at the same temporal and spatial scale as observations. The best models are selected for analyzing the changes in the triennial oscillation in future projections. The selection of best models is made by the following procedure:

Step 1: The significant triennial oscillation in each grid for all models is extracted. That is,

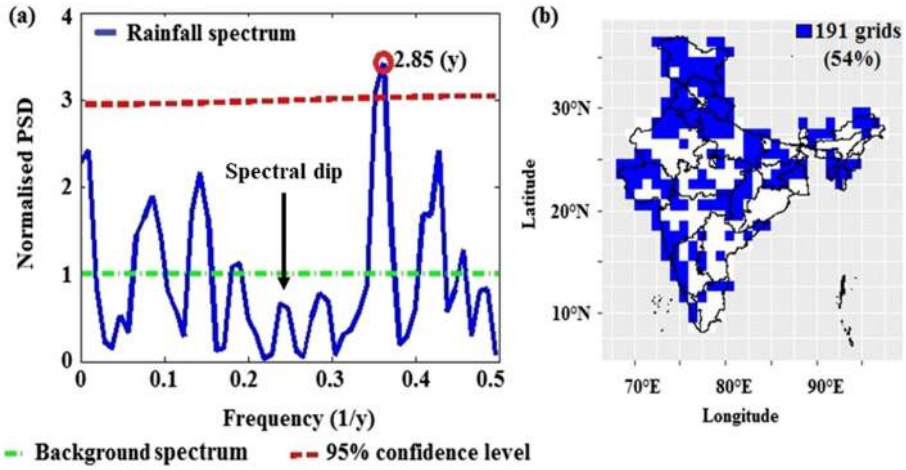

Figure 1. (a) Indian summer monsoon rainfall spectrum obtained from Welch technique and the background spectrum (dashed horizontal line) with 95% confidence levels. Period (year) is marked at a significant peak; (b) spatial distribution of 95% significant triennial oscillation. PSD = power spectral density.

$$PSD\left[M_{i,j}\right], i = 1, 2, 3, \ldots 28 \quad \& \quad j = 1, 2, 3, \ldots 354. \tag{6}$$

i identifies the model used among the 28 models selected, whereas *j* indicates the grid number corresponding to the spatial location at which the PSD is being evaluated. Here $[M_{i,j}]$ represents *i*th models and *j*th location.

Step 2: It extracts the spatial locations *j* at which observed periodicity match with model value.

$$PSD\left[M_{i,j}\right] = PSD\left[obs_j\right] \tag{7}$$

That is, it identifies the grid points, where both observation and model have the same periodicity.

Step 3: Then for the *i*th model, the grid numbers at which model and observation agree are collected.
Step 4: The 75th percentile value of the collected grids of all models is calculated. This value is considered as threshold (*ths*) value for acceptance to filter out the model.
Step 5: M_i is selected if $M_{i,j} \geq ths$.

Based on the above criteria, the result obtained from the model MIROC-ESM-CHEM matches 74% with the observations, which is highest in comparison with others, followed by the HadGEM2-ES (69% matching). The spatial matching of observations with five models, namely, MIROC-ESM-CHEM (74%), HadGEM2-ES (69%), MPI-ESM-LR (64%), MIROC-ESM (57%), and IPSL-CM5A-MR (57%) is shown in Figure 2. These five models have triennial oscillation in 40%, 37%, 31%, 31%, and 37% grids, respectively, and are selected for future projections. Furthermore, Figure 3 shows the grid points at which more than three models agree with observations. It is found that 73% of the model grids match with the observations as depicted in Figure 3.

It is also equally important to analyze all-India triennial oscillation of the selected models for the hind-cast time period. The results are depicted in Figure 4 and are in corroboration with the observations. Therefore, these five models, namely, MIROC-ESM-CHEM, HadGEM2-ES, MPI-ESM-LR, MIROC-ESM, and IPSL-CM5A-MR, are considered for future analysis.

The PSD of projected all-India rainfall over 2005–2100 of the selected models are estimated for ISMR time series. The results depicted in Figure 5 reveal that the confidence level of the triennial oscillation of the two models, MIROC-ESM-CHEM and IPSL-CM5A-MR, are above the 95%, whereas a shift in the confidence level is detected by three models out of the five. It is found that the confidence level of the triennial oscillation reduces to 85% from 95%, in the model HadGEM2-ES and MPI-ESM-LR, whereas the confidence level is reduced to 90% in the model MIROC-ESM.

So as to examine the changes in the spatial pattern of the triennial oscillation at the regional scale, the PSD function is implemented for projected gridded rainfall of the selected models. Results reveal that the confidence level of the triennial oscillation is likely to shift from higher to lower levels. The total number of grids,

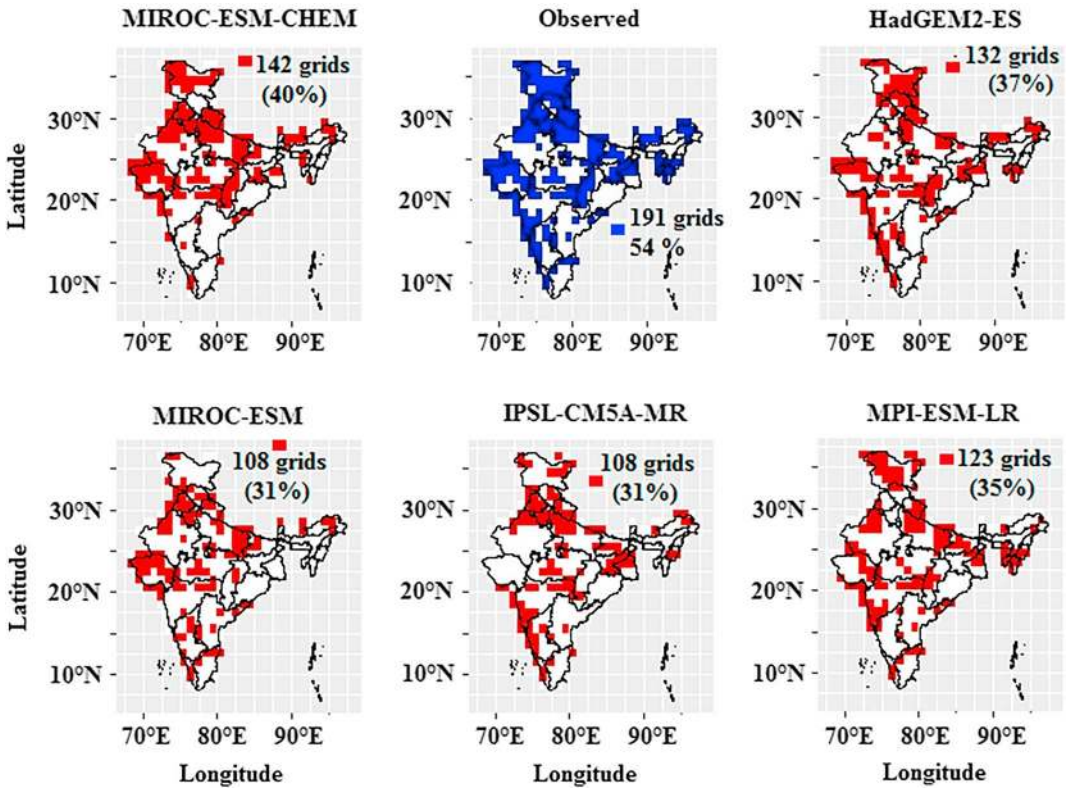

Figure 2. The spatial matching of five best models with the observations.

in which a change in the confidence level from historical to projections is seen, has been estimated and is shown in Figure 6. It is revealed that, in the model HadGEM2-ES, the confidence level has reduced in 70% of the significant grids, which is the highest in comparison with other selected models. It is followed by the model IPSL-CM5A-MR (65%), whereas such transformation is seen least in the model MIROC-ESM-CHEM. Percentage shown in each of the models in Figure 6 indicates the decrease in confidence level from higher to lower of the triennial oscillation. Furthermore, it counts the spatial grids in which such changes have been encountered.

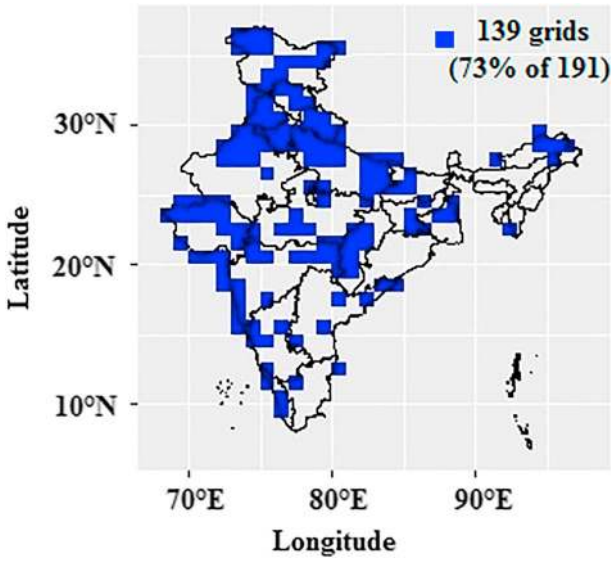

Figure 3. The spatial distribution of triennial oscillation of ISMR at which model's agreement matches with the observations.

However, the spatial patterns of the triennial oscillation projections seem to be different among the selected models. To identify the unique geographical locations based on the selected model's agreement, Figure 7 is brought into the picture to clearly estimate the changes in the triennial oscillation and to visualize the sensitive region which could experience such changes. Figure 7a represents significant triennial oscillation of the selected models based on the maximum agreement in historical time period. It is shown that the 139 grids out of 191 (73%) match with the observations (see Figure 1b).

Figure 7b represents the distribution of triennial oscillation, which is significant at lower confidence level (below 95%) in future projections. The result, as shown in the figure, clearly indicates that the confidence level of the triennial oscillation reduces in 80% of the grids (which is 112 grids out of 139). The results suggest that the regions of southwest-coast, northern, and northeast-central India experience such changes. The southwest-coastal region of India assumes its importance due to the Western Ghats. It is widely reported that Western Ghats, India's largest

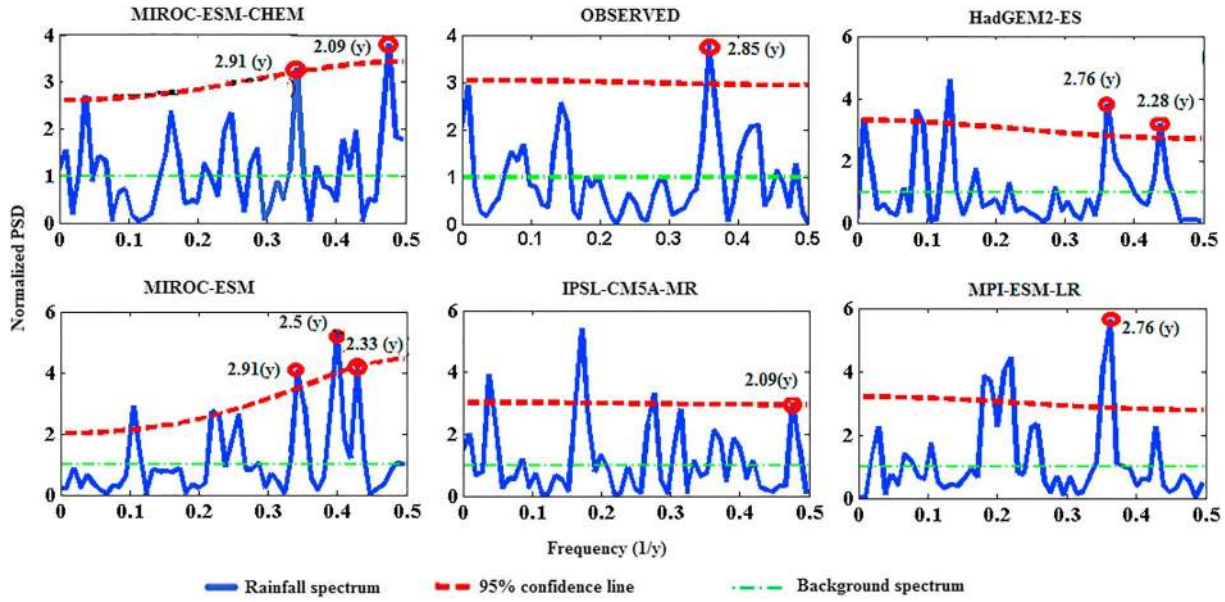

Figure 4. The power spectral density (PSD) of Indian summer monsoon rainfall in the historical time period of Coupled-Model Inter-comparison Project Phase 5 models (1901–2005).

natural carbon, sinks and a biodiversity hot spot has been adversely affected due to climate change (Manjunatha et al., 2015; Murugan et al., 2009). Also, in southwest-coastal region temperature hot spots have been identified in Narula et al. (2018) where it has been shown the region undergoes several mean change years in average temperature. The change in the strength of triennial oscillation could be due to the changes in temperature over south-coast region. The regions of northeast-central and northern part of India are known to be rich in agricultural products, which depend on abundant

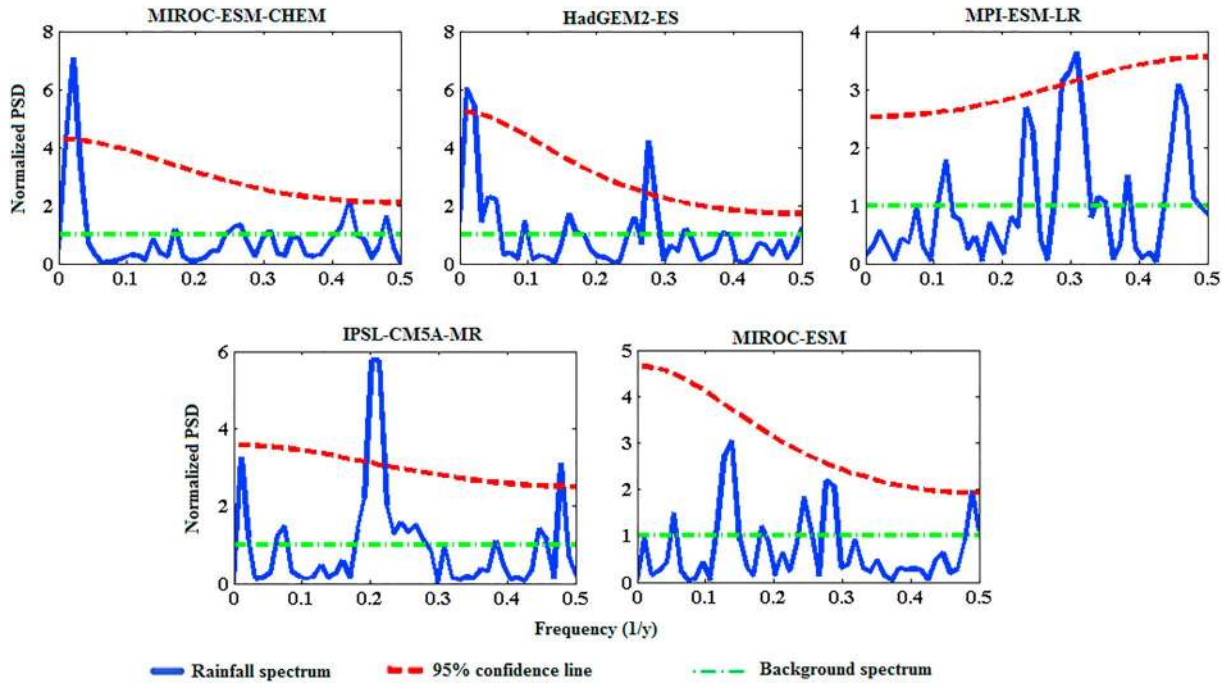

Figure 5. The power spectral density (PSD) of Indian summer monsoon rainfall in the projected time period of Coupled-Model Inter-comparison Project Phase 5 models (2005–2100).

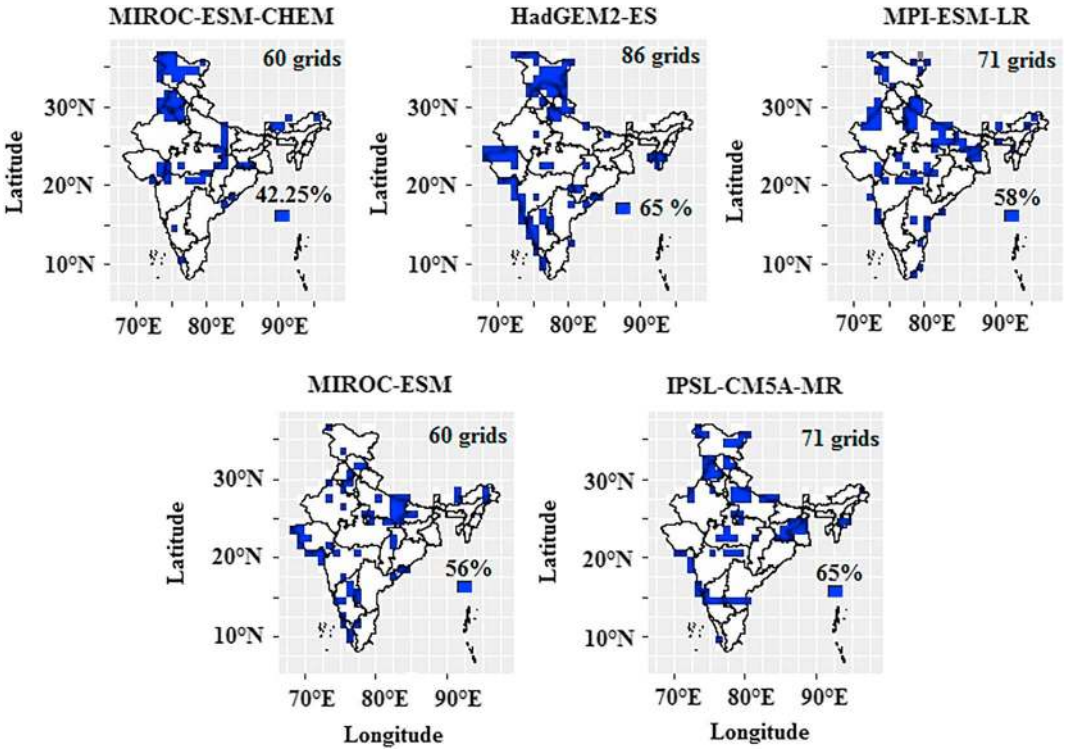

Figure 6. Spatial pattern of the triennial oscillation of the selected Coupled-Model Inter-comparison Project Phase 5 model's projection.

rainfall (Prasanna, 2014). This could severely threaten the lives of those depending on agricultural products and agribusiness industry.

The confidence level of the triennial oscillation in the future projections is reduced to lower levels, and their spatial distribution is shown in Figure 7c, whereas the exact number of grids for various confidence levels are shown in Figure 7d. It shows that the confidence level of the triennial oscillation is reduced to 80%, 85%, and 90%, respectively, in 3%, 20%, and 62% of the grids, respectively, whereas about 15% of the grids experience triennial oscillation below 95% confidence level. This indicates the weakening of the triennial oscillation in amplitude over large parts of the country.

The analysis so far has been performed in the frequency domain; we now aim to establish the significance of our result in the time domain. This is performed by establishing a one-to-one correspondence in time and frequency domain. For this purpose, a statistical procedure is explained as follows: First, Student's t test is implemented to check whether the mean rainfall of projections has significantly decreased in comparison to historical data. The test is implemented separately on the all-India and gridded data. The null hypothesis is defined as $H_0 : \mu_1 = \mu_2$, where μ_1, μ_2 represent the mean rainfall of historical and projected models, respectively, with alternate hypothesis defined as $H_1 : \mu_2 < \mu_1$. Hence, the rejection of null hypothesis would imply that the amount of the mean rainfall of projections is significantly less than historical data.

The results reveal that the null hypothesis is rejected at 5% significance level ($p < 0.001$) for all the five models, which indicates that the mean rainfall of the projected models is indeed significantly less than the historical data. Similarly, same statistical test is applied on regional scale, and the hypothesis is rejected over the grids where confidence level of the triennial oscillation is significantly reduced. Specifically, it is seen that the mean rainfall of model's projections of all grids is decreased in time domain, where the triennial oscillation has reduced its confidence level to 80% in frequency domain. Furthermore, mean rainfall of projections has significantly decreased in 65.7% and 63.6% of the grids, where the confidence levels of the oscillation have reduced to 90% and 85%, respectively. Hence, it is concluded that the mean rainfall of projections is significantly less in comparison to historical data.

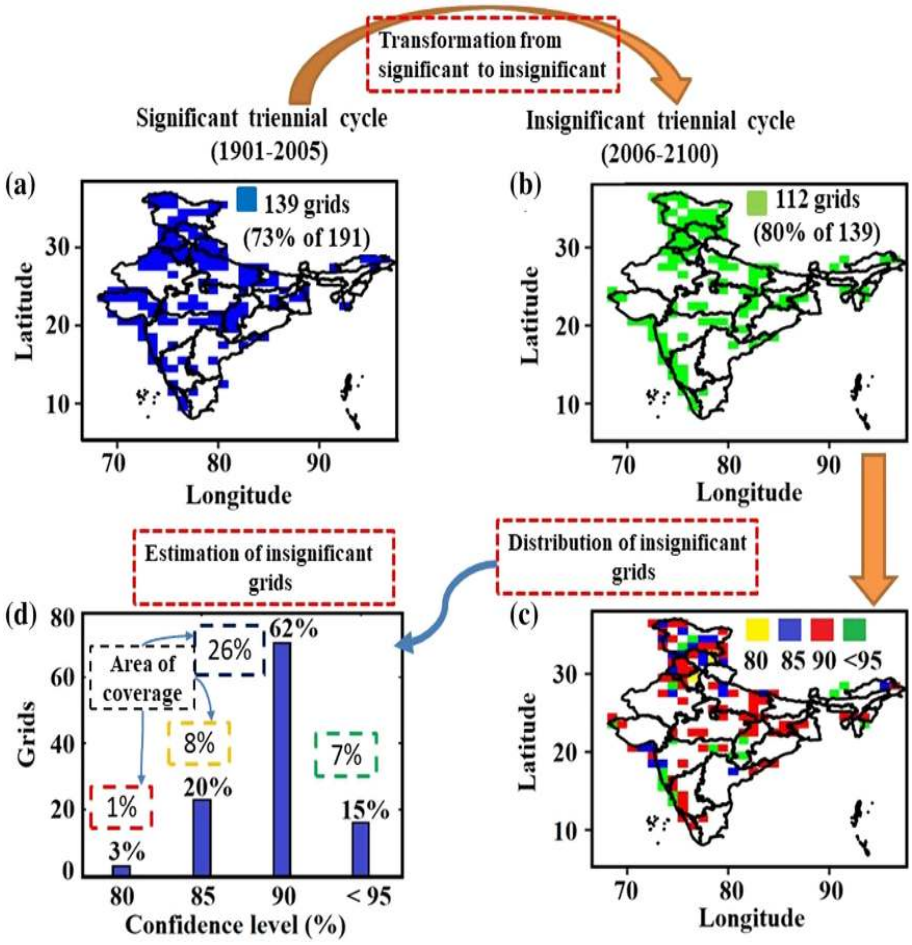

Figure 7. Changing spatial pattern of the confidence level of triennial oscillation at the gridded level (a) significant triennial oscillation in the historical simulations (1901–2005); (b) triennial oscillation in the projections that have changed their significance levels; (c) confidence levels of changed grids; (d) estimated number of grids where significance levels are changed. The area under insignificant grids is also mentioned along with the percentage of changed grids.

In order to further check the strength of each cycle in time domain, the corresponding years are extracted using equations (1) and (2). Then after, the conditional probability of each cycle is calculated for historical and projected models over time. Mathematically, it is defined as follows:

$$P = P(T \leq \mu | (\text{Eq.1 or Eq.2})), i = t_1, ...t_n, \tag{8}$$

where μ represents the long-term mean of rainfall; t_1,.....t_n represent years; and the value of n is 105 and 94 for historical and projections, respectively. The cyclic mean T is calculated by taking the average of three consecutive years, which satisfies either equation (1) or (2). From the analysis, it is concluded that the strength of triennial cycle is likely to reduce in most of the selected projected models with probability as high as 93.65%.

4. Summary and Discussions

Many studies have been performed on the periodicity detection, mainly focusing on all-India index and homogenous zones. The gridded data, however, have not been subjected to periodicity detection. Interestingly, in this study we find that the significant triennial oscillation (at 95% confidence level) is present over 54% of the observed grids, which is 69.03% of the total area. This forms a dense cluster above the 26° latitude (northern India), whereas sparsely distributed significant grids are seen below 18° latitude (southern India). Moreover,

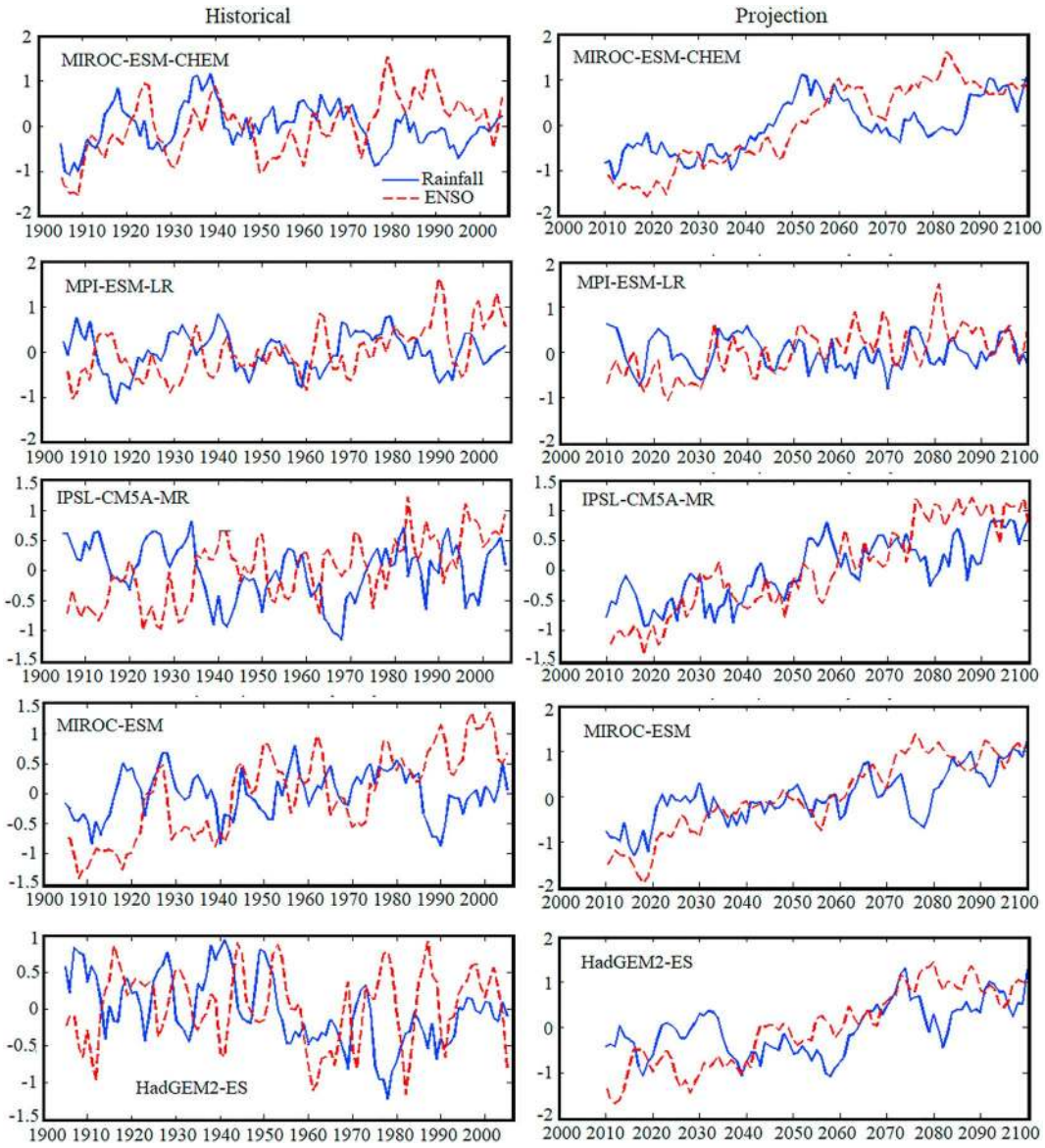

Figure 8. Normalized moving average of June to September annual rainfall and El Niño Southern Oscillation (ENSO) of the selected models over historical and projection time period.

an elongated strip of significant grids is less densely distributed from western to northeast India (in between 18° and 26° latitude). Further, our results revealed that 5 CMIP5 models out of 28, namely, MIROC-ESM-CHEM, HadGEM2-ES, MIROC-ESM, MPI-ESM-LR, and IPSL-CM5A-MR, capture the behavior of triennial oscillation both at all-India and gridded scale. To consolidate the results of these five models, an integrated form is obtained, which displays a remarkable degree of spatial similarity with the observations based on the maximum matching of all models at the gridded scale. Projections disclose that the confidence levels of the triennial oscillation will reduce over large parts of the country. In particular, it is demonstrated that the triennial oscillation at 95% confidence level is preserved only in 20% and the remaining 80% of the selected grids, which covers 41.3% area is likely to be insignificant in future projections. The southwest-coastal, northern, and northeast-central part of India will mainly experience changes where confidence levels of the triennial oscillation are projected to reduce from 95% to up to 80%.

This weakening of the triennial oscillation (in amplitude) of Indian monsoon rainfall is investigated further and demonstrated in Figure 8. It represents the normalized ENSO index against JJAS rainfall. The result

presented in Figure 8 suggests that high positive index of ENSO corresponds to low negative index of ISMR and vice versa. This indeed explains the inverse relation between ISMR and ENSO in time domain, which has been established in frequency domain in Azad and Rajeevan (2016). Furthermore, it is observed in Figure 8 that the cycle of rainfall and ENSO, which is evident in the historical time period, seems to be changing in model's projections. Although the inverse relation is preserved in future time domain, abrupt changes in ISMR indicate the influence of nonlinear forcing such as ENSO.

It can be deduced from this inverse relation that ENSO acts as a driving force to modulate ISMR. However, some of ENSO episodes enhance while some other diminish ISMR. So it is required to quantify the role of ENSO during strong and weak triennial oscillation. Therefore, in addition, strong and weak triennial cycles are extracted using equations (1) and (2) over the time 2006–2100. Then corresponding ENSO index is also extracted to quantify the inverse relation in triennial cycle band. Further, it also gives probabilistic measure whether triennial cycle is affected by the ENSO cycle. The study reveals that there is 58% of chance of weak ENSO cycle persists in active phase of triennial cycle and 52% of chance of strong ENSO cycle in weak phase of triennial cycle.

To conclude, we summarize that the weakening of the triennial oscillation of ISMR depends on the global phenomenon ENSO. Azad and Rajeevan (2016) have presented evidence of a possible shift of Indian monsoon rainfall-ENSO inverse relation toward shorter time periods (3–2.5 years) in the future. In response to this change, the present paper has evaluated the significance of the triennial oscillation in future projections and revealed that the confidence level of this oscillation are likely to decrease over a large part of the country.

Water resource management, which is dependent on the monsoon, is highly critical for the Indian subcontinent. The results of this study can be used to prepare for social, agricultural, and economic conditions resulting from strong and weak monsoons.

Acknowledgments
Authors are very grateful to Prof. Roddam Narasimha (FRS), Jawaharlal Nehru Centre for Advanced Scientific Research, Bangalore, for the valuable comments and suggestions on the manuscript. The observed and CMIP5 model's rainfall gridded data are obtained from the open web repositories of Climate Research Unit, UK (http://www.cru.uea.ac.uk and http://pcmdi9.llnl.gov/, respectively).

References

Accadia, C., Mariani, S., Casaioli, M., Lavagnini, A., & Speranza, A. (2003). Sensitivity of precipitation forecast skill scores to bilinear interpolation and a simple nearest-neighbor average method on high-resolution verification grids. *Weather and Forecasting*, *18*(5), 918–932.

Azad, S., & Narasimha, R. (2008). A wavelet based significance test for periodicities in Indian monsoon rainfall. *International Journal of Wavelets, Multiresolution and Information Processing*, *6*(2), 291–304.

Azad, S., Narasimha, R., & Sett, S. K. (2007). Multiresolution analysis for separating closely spaced frequencies with an application to Indian monsoon rainfall data. *International Journal of Wavelets, Multiresolution and Information Processing*, *5*(05), 735–752.

Azad, S., & Rajeevan, M. (2016). Possible shift in the ENSO-Indian monsoon rainfall relationship under future global warming. *Scientific Reports*, *6*, 20145.

Azad, S., Vignesh, T. S., & Narasimha, R. (2010). Periodicities in Indian monsoon rainfall over spectrally homogeneous regions. *International Journal of Climatology*, *30*(15), 2289–2298.

Chaudhari, H. S., Shinde, M. A., & Oh, J. H. (2010). Understanding of anomalous Indian summer monsoon rainfall of 2002 and 1994. *Quaternary International*, *213*(1-2), 20–32.

Feng, X., Porporato, A., & Rodriguez-Iturbe, I. (2013). Changes in rainfall seasonality in the tropics. *Nature Climate Change*, *3*(9), 811.

Gilman, D. L., Fuglister, F. J., & Mitchell, J. J. (1963). On the power spectrum of "Rednoise". *Journal of the Atmospheric Sciences*, *20*, 182–184.

Harris, I., Jones, P. D., Osborn, T. J., & Lister, D. H. (2014). Updated high-resolution grids of monthly climatic observations–the CRU TS3 10 dataset. *International Journal of Climatology*, *34*(3), 623–642.

Iyengar, R. N., & Kanth, S. R. (2005). Intrinsic mode functions and a strategy for forecasting Indian monsoon rainfall. *Meteorology and Atmospheric Physics*, *90*(1-2), 17–36.

Jena, P., Azad, S., & Rajeevan, M. N. (2015). Statistical selection of the optimum models in the CMIP5 dataset for climate change projections of Indian monsoon rainfall. *Climate*, *3*(4), 858–875.

Jena, P., Azad, S., & Rajeevan, M. N. (2016). CMIP5 projected changes in the annual cycle of Indian monsoon rainfall. *Climate*, *4*, 14.

Kailas, S. V., & Narasimha, R. (2000). Quasi cycles in monsoon rainfall using wavelet analysis. *Current Science*, *78*, 592–595.

Knutti, R., & Sedláček, J. (2013). Robustness and uncertainties in the new CMIP5 climate model projections. *Nature Climate Change*, *3*(4), 369–373.

Kociuba, G., & Power, S. B. (2015). Inability of CMIP5 models to simulate recent strengthening of the walker circulation: Implications for projections. *Journal of Climate*, *28*(1), 20–35.

Kripalani, R. H., Kulkarni, A., Sabade, S. S., & Khandekar, M. L. (2003). Indian monsoon variability in a global warming scenario. *Natural Hazards*, *29*(2), 189–206.

Kumar, K. (1997). Seasonal forecasting of Indian summer monsoon rainfall: Diagnostics and synthesis of regional and global signals, (Ph.D thesis, University of Pune).

Liu, Y., Hu, Z. Z., Kumar, A., Peng, P., Collins, D. C., & Jha, B. (2015). Tropospheric biennial oscillation of summer monsoon rainfall over East Asia and its association with ENSO. *Climate Dynamics*, *45*(7-8), 1747–1759.

Loschnigg, J., Meehl, G. A., Webster, P. J., Arblaster, J. M., & Compo, G. P. (2003). The Asian monsoon, the tropospheric biennial oscillation, and the Indian Ocean zonal mode in the NCAR CSM. *Journal of Climate*, *16*(11), 1617–1642.

Manjunatha, B. R., Balakrishna, K., Krishnakumar, K. N., Manjunatha, H. V., Avinash, K., Mulemane, A. C., & Krishna, K. M. (2015). Increasing trend of rainfall over Agumbe, Western Ghats, India in the scenario of global warming. *The Open Oceanography Journal*, *8*(1).

Meehl, G. A. (1987). The annual cycle and interannual variability in the tropical Pacific and Indian Ocean regions. *Monthly Weather Review*, *115*(1), 27–50.
Meehl, G. A. (1997). The south Asian monsoon and the tropospheric biennial oscillation. *Journal of Climate*, *10*(8), 1921–1943.
Meehl, G. A., & Arblaster, J. M. (2002). The tropospheric biennial oscillation and Asian–Australian monsoon rainfall. *Journal of Climate*, *15*(7), 722–744.
Meehl, G. A., Arblaster, J. M., & Loschnigg, J. (2003). Coupled ocean–atmosphere dynamical processes in the tropical Indian and Pacific Oceans and the TBO. *Journal of Climate*, *16*(13), 2138–2158.
Menon, A., Levermann, A., Schewe, J., Lehmann, J., & Frieler, K. (2013). Consistent increase in Indian monsoon rainfall and its variability across CMIP-5 models. *Earth System Dynamics*, *4*, 287–300.
Mooley, D. A., & Parthasarathy, B. (1984). Fluctuations in all-India summer monsoon rainfall during 1871–1978. *Climatic Change*, *6*(3), 287–301.
Murugan, M., Shetty, P. K., Anandhi, A., Ravi, R., Alappan, S., Vasudevan, M., & Gopalan, S. (2009). Rainfall changes over tropical montane cloud forests of southern Western Ghats, India. *Current Science*, 1755–1760.
Narasimha, R., & Bhattacharya, S. (2010). A wavelet cross-spectral analysis of solar–ENSO–rainfall connections in the Indian monsoons. *Applied and Computational Harmonic Analysis*, *28*(3), 285–295.
Narula, P., Sarkar, K., & Azad, S. (2018). A functional evaluation of the spatiotemporal patterns of temperature change in India. *InternationalJournal of Climatology*, *38*(1), 264–271.
Prasanna, V. (2014). Impact of monsoon rainfall on the total food grain yield over India. *Journal of Earth System Science*, *123*(5), 1129–1145.
Rajeevan, M., Bhate, J., Kale, J. D., & Lal, B. (2006). High resolution daily gridded rainfall data for the Indian region: Analysis of break and active. *Current Science*, *91*(3), 296–306.
Sengupta, A., & Rajeevan, M. (2013). Uncertainty quantification and reliability analysis of CMIP5 projections for the Indian summer monsoon. *Current Science*, *105*(12), 1692–1703.
Spicer, R. A., Valdes, P. J., Spicer, T. E. V., Craggs, H. J., Srivastava, G., Mehrotra, R. C., & Yang, J. (2009). New developments in CLAMP: Calibration using global gridded meteorological data. *Palaeogeography, Palaeoclimatology, Palaeoecology*, *283*(1-2), 91–98.
Stoica, P., & Moses, R. L. (1997). *Introduction to spectral analysis*. New Jersey: Prentice Hall.
Taylor, K. E., Stouffer, R. J., & Meehl, G. A. (2012). An overview of CMIP5 and the experiment design. *Bulletin of the American Meteorological Society*, *93*, 485–498.
Yoon, S. S., Phuong, A. T., & Bae, D. H. (2012). Quantitative comparison of the spatial distribution of radar and gauge rainfall data. *Journal of Hydrometeorology*, *13*(6), 1939–1953.